

## Prediction of surface roughness and delamination in end milling of GFRP using mathematical model and ANN

P Praveen Raj<sup>a\*</sup>, A Elaya Perumal<sup>b</sup> & P Ramu<sup>a</sup>

<sup>a</sup>Department of Mechanical Engineering, Thanthai Periyar Government Institute of Technology,  
Bagayam, Vellore 632 002, India

<sup>b</sup>Engineering Design Divisions, Department of Mechanical Engineering, College of Engineering Guindy,  
Anna University, Chennai 600 025, India

*Received 29 March 2011, accepted 12 March 2012*

Glass fiber reinforced plastics (GFRP) composite is considered to be an alternative to heavy exortic materials. Accordingly, the need for accurate machining of composites has increased enormously. During machining, the reduction of delamination and obtaining good surface roughness is an important aspect. The present investigation deals with the study and development of a surface roughness and delamination prediction model for the machining of GFRP plate using mathematical model and artificial neural network (ANN) multi objective technique. The mathematical model is developed using RSM in order to study main and interaction effects of machining parameters. The competence of the developed model is verified by using coefficient of determination and residual analysis. ANN models have been developed to predict the surface roughness and delamination on machining GFRP components within the range of variables studied. Predicted values of surface roughness and delamination by both models are compared with the experimental values. The results of the prediction models are quite close with experiment values. The influences of different parameters in machining GFRP composite have been analyzed.

**Keywords:** ANOVA, Glass fiber reinforced plastics, End milling, Response surface methodology, Artificial neural network, Multi-objective techniques

Glass fiber reinforced plastic (GFRP) composites are most widely used in aerospace, automobile and marine industries owing to their potential properties such as a high strength to weight ratio, and high specific stiffness. The machining of GFRP has necessitated manufacturing near net-shaped components. The machining of a composite is different from the conventional machining of metals due to the composites anisotropic and non homogeneous nature. Among several industrial machining processes, milling is a fundamental machining operation. End milling is the most common metal removal operation encountered. It is widely used in a variety of manufacturing industries including the aerospace and automotive sectors, where quality is an important factor in the production of slots and dies. The quality of the surface plays a very important role in the performance of milling as a good-quality milled surface significantly improves fatigue strength, corrosion resistance and creep life. Surface roughness also affects several functional attributes of parts, such as wearing, heat transmission, and ability of holding a lubricant,

coating, or resisting fatigue. Therefore, the desired surface finish is usually specified and the appropriate processes are selected to reach the required quality. Several factors influence the final surface roughness in end milling operation<sup>1,2</sup>.

Surface roughness is a characteristic that could influence the dimensional precision, the performance of the mechanical pieces and production cost. For these reasons there has been a lot of research and development with the objectives of optimizing cutting conditions to obtain a determined surface roughness<sup>3,4</sup>.

Because of the inhomogeneous nature of composite materials, their response to machining may involve undesirable consequences such as rapid tool wear, fiber pullout, surface burning and smearing, pitting and delamination. All of these responses are directly related to the cutting tool force applied to the work piece edge. Delamination in particular is strongly dependent on the cutting parameter component normal to the stacking plane in unidirectional and multidirectional laminate composites. The delamination of fibers from matrix due to excessive cutting parameter is a major problem in machining, which results in the lowering of bearing strength and

\*Corresponding author (E-mail: ppraj\_tpgit@rediffmail.com)

is detrimental to the durability by reducing the in-service life under fatigue loads<sup>1,2</sup>.

Several optimization techniques, which can be classified as conventional and non-conventional (soft computing), could be effectively applied to optimize the cutting conditions that affect the surface roughness ( $R_a$ ) value. The conventional optimization techniques include Taguchi method, factorial technique and response surface methodology (RSM). Among the conventional optimization techniques, RSM was mostly applied by researchers<sup>5</sup>.

The selection of efficient machining parameters is of great concern in manufacturing industries, where economy of machining operations plays a key role in the competitive market. Many researchers have dealt with the optimization of machining parameters. The RSM is a dynamic and foremost important tool of design of experiment (DOE) where in the relationship between process output(s) and its input decision variables, it is mapped to achieve the objective of maximization or minimization of the output properties. RSM was successfully applied for prediction and optimization of cutting parameters<sup>5,6</sup>.

Modeling of manufacturing process and optimization are two major issues in metal cutting optimization. In order to develop surface roughness model and optimizing the process it is essential to review the published literature for understanding current status of work in this area. Hasmi *et al.*<sup>7</sup> used the RSM model for assessing the influence of the work piece material on the surface roughness on steel specimen. They establish the relationship between surface roughness and cutting parameters, viz., cutting speed, feed and depth of cut. Alauddin *et al.*<sup>8</sup> established a mathematical model for predicting the surface roughness of 190 BHN steel using end milling processes. They developed the prediction model using response surface methodology to predict surface roughness in term of cutting speed, feed rate and depth of cut. Reddy and Rao<sup>9</sup> studied the influence of tool geometry during end milling of medium carbon steel using RSM and the model is optimized with genetic algorithm to obtain minimum surface roughness and the corresponding cutting conditions.

Lou and Chen<sup>10</sup> studied the effect of spindle speed, feed rate and depth of cut on the surface roughness of end milling processes. They used in-process surface roughness recognition (ISRR) and a neural fuzzy system for predicting work piece surface roughness.

Chiang *et al.*<sup>11</sup> developed a scheme for evaluation of optimal cutting condition using two different kinds of

neural networks. They used a neural network that works on back propagation algorithm, having three inputs and four outputs to simulate the machining process. The second network is used to calculate the optimal cutting parameters to achieve the goal of maximizing the material removal rate. Luo *et al.*<sup>12</sup> developed a neural network to simulate the cutting force and contour error in an end milling process. The neural network is used to make corrections to the feed rate components with parametric interpolation algorithm so as to minimize the contour error caused by the dynamic lag of the closed-loop servo systems used to control the table feed drives. Rangwala and Dornfeld<sup>13</sup>, Kohli and Dixit<sup>14</sup> and many others used artificial neural network models for predicting surface roughness in a turning process with different network training methodology and input parameters.

Survey of previous research on surface roughness prediction in end milling process reveals that most of the researchers used mathematical model, multiple regression method, response surface methodology, the fuzzy-set based technique and neural network are various popular prediction techniques<sup>14,15</sup>. Chandrasekaran *et al.*<sup>16</sup> carried out the review of previous research about the application of soft computing methods on parameter prediction such as surface roughness, tool life and tool wear, cutting force, etc., including process optimization for four common machining processes. Among this, neural network modeling seems to be more promising method for predicting surface finish with reasonable accuracy with lesser computational time.

The objective of this paper is to develop a mathematical model for prediction of surface roughness and delamination of a GFRP subjected to end milling using coated and uncoated K10 end mills under various cutting conditions. The mathematical model was developed using response surface methodology and prediction model was developed using artificial neural network multi objective technique. The design of experiment and the prediction of surface roughness and delamination values were done using response surface methodology and artificial neural network – multi objective technique. Both the techniques were developed as the adaptability of the industries varies.

## Experimental Procedure

### Materials and experimental set-up

The GFRP plate is fabricated with one layer of glass fiber in the form of woven row mat reinforced

between two layers of plastic. Likewise eight layered unidirectional GFRP specimens of 6.5 mm thickness were prepared using the hand lay-up process. The reinforcement was in the form of unidirectional E-glass fiber tape and matrix was epoxy, Araldite LY556 with hardener HY 951 (Aliphatic primary amine) was used for the fabrication. A gel coat was applied on the mould prior to the lay-up process to facilitate easy removal of the laminate. Specimens were cured at room temperature having a fiber orientation of 0/90°. Figure 1 shows the glass fiber used for reinforcement in the form of woven row mat (w.r.m) and Fig. 2 shows the fabricated plate.

The tools that were chosen for milling were K10 end mills of solid carbide, and solid carbide end mill coated with titanium nitride (Ti Namite) and

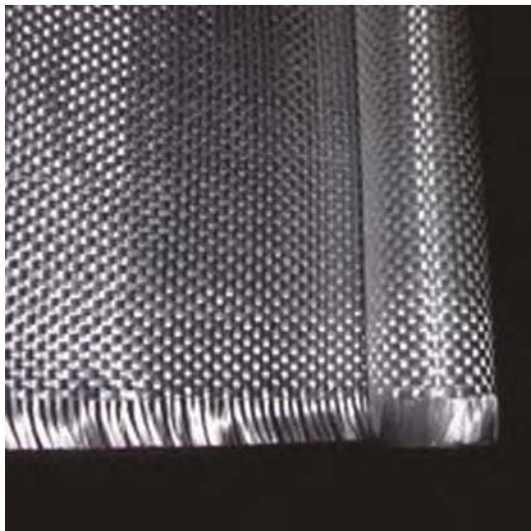


Fig. 1—Glass fiber in the form of woven roving mat



Fig. 2—The fabricated GFRP plate

aluminium titanium nitride (TiNamite A) having four flute each with square ends. The tool has 30° right hand spiral with centre cutting. The factors were set depending upon their micro-hardness levels. The tools used for the study is SGS carbide make. The milling operation was conducted using a universal milling machine with a spindle speed of 45-1400 m/min, longitudinal feed of 18 mm/min and cross feed range of 16-800 mm/min. The machine has a vertical feed of 6.3-315 m/min and a clamping area of 300 × 1000 mm. The fixation of the composite material was made in such a way so as to eliminate the vibration and displacement. The specifications of the machine are shown in Table 1.

**Design of experiment**

The cutting speed  $v$  (m/min), feed  $f$  (mm/min), depth of cut  $d$  (mm) and tool material  $T$  are the four parameters under investigation in the present study. A full factorial experimental design with a total of 27 experiment runs was carried out. The factors and respective levels are shown in Table 2. The surface roughness and delamination were the response variable recorded for each run. The treatment of experimental result is based on the analysis of variance (ANOVA). The analysis of variance of the experimental data for the surface roughness and delamination generated during end milling of GFRP is done to study the relative significance of the cutting speed, feed, depth of cut and tool material.

**Response surface methodology**

In statistics, response surface methodology explores the relationships between several explanatory variables and one or more response. The main idea of RSM is to

Table 1—Machine specifications

Work clamping area	300 × 1000 mm
Spindle speed	45 - 1400 m/min
Longitudinal and cross feed range	18, 16 - 800 mm/min
Vertical feed	18, 6.3 - 315 m/min

Table 2—Factors and their levels

Factors	Notation used	Levels		
		-1	0	1
Cutting speed (m/min)	A	100	700	1300
Feed (mm/min)	B	50	350	650
Depth of cut (mm)	C	1	2	3
Tool material	D	Solid carbide	Titanium Nitride coated	Aluminium titanium nitride coated

use a sequence of design to obtain an optimal response. Box and Wilson<sup>17</sup> suggest using a second-degree polynomial model to do this. They acknowledge that this model is only an approximation, but it is easy to estimate and apply, even when little is known about the process.

An easy way to estimate a first-degree polynomial model is to use a factorial experiment or a fractional factorial designs. This is sufficient to determine which explanatory variables have an impact on the response variable(s) of interest. Once it is suspected that only significant explanatory variables are left, and then a more complicated design, such as a central composite design can be implemented to estimate a second-degree polynomial model, which is still only an approximation at best. However, the second-degree model can be used to optimize (maximize, minimize, or attain a specific target) a response.

Some extensions of response surface methodology deal with the multiple response problem. Multiple response variables create difficulty because what is optimal for one response may not be very optimal for other responses. Other extensions are used to reduce variability in a single response while targeting a specific value, or attaining a near maximum or minimum while preventing variability in that response from getting too large.

There are two types of response surface designs central composite design and Box-Behnken design. The study uses the Box-Behnken design in the optimization of experiments using RSM to understand the effect of important parameters. Box-Behnken design is normally used when performing non-sequential experiments. That is, performing the experiment only once. These designs allow efficient estimation of the first and second –order coefficients. Because Box-Behnken design has fewer design points, they are less expensive to run than central composite designs with the same number of factors. Box-Behnken design do not have axial points, thus we can be sure that all design points fall within the safe operating zone. Box-Behnken design also ensures that all factors are never set at their high levels simultaneously. Table 3 shows the Box-Behnken design used for conducting the experiment.

Table 3—Box-Behnken design

Factor	Replicati on	Base runs	Total runs	Base block	Total block	Center point
4	1	27	27	1	1	3

To investigate how process parameters affect on process state variables (i.e. surface roughness and delamination), experiments were conducted using Box-Behnken design using three levels and four factors. The feed rate, spindle speed, depth of cut and tool materials considered as independent input variables. Linear and second order polynomials were fitted to the experimental data for obtaining the regression equations. The lack of fit test, variance test and other adequacy measures were used in selecting optimum models. The proposed linear model correlating the responses and independent variables can be represented by the following expression:

$$y = \beta_0 x_0 + \beta_1 x_1 + \beta_2 x_2 + \beta_3 x_3 + \beta_4 x_4 \quad \dots (1)$$

where y is the response and C is constants. Eq. (1) can be written as:

$$Y = \beta_0 + \sum_{i=1}^k \beta_i X_i + \sum_{i=1}^k \beta_{ii} X_i^2 + \sum_{i=1}^{k-1} \sum_{j=i+1}^k \beta_{ij} X_i X_j \quad \dots (2)$$

Where y is the response,  $x_0 = 1$ (dummy variable),  $x_1$ = cutting speed,  $x_2$  = feed rate, and  $x_3$  = depth of cut and  $x_4$  = tool material,  $\beta_0 = C$  and  $\beta_1, \beta_2, \beta_3$  and  $\beta_4$  are the model parameters.

**Measurements of surface roughness**

Surface roughness is the measure of finer surface irregularities in the surface texture. These are the result of the manufacturing process employed to create the surface. Surface roughness  $R_a$  is the arithmetic average deviation of the surface valleys and peaks expressed in micro inches or micro meters. ISO standards use the term CLA (center line average). Both are interpreted in an identical way.

The ability of a manufacturing operation to produce a specific surface roughness depends on many factors. For example, in end mill cutting, the final surface depends on the rotational speed of the end mill cutter, the velocity of the traverse, the rate of feed, the amount and type of lubrication at the point of cutting, and the mechanical properties of the piece being machined. A small change in any of the above factors can have a significant effect on the surface produced. A surface consists of three basic components: form, waviness and roughness.

Surface roughness is measure of texture of a surface. It is quantified by the vertical deviations of a real surface form its ideal form. If theses deviations

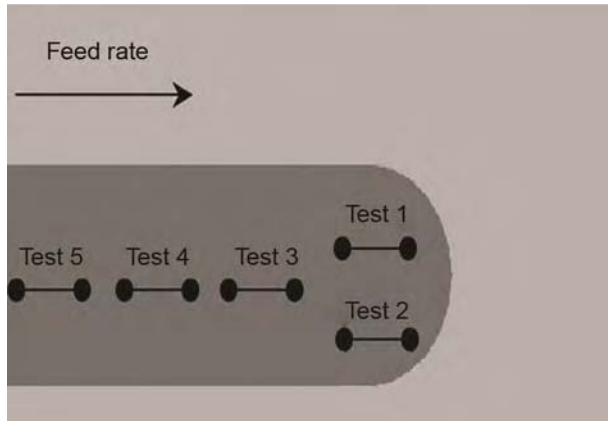


Fig. 3—Measurements of surface roughness were made with the cut-off 0.8mm according to ISO at five different sample test points.

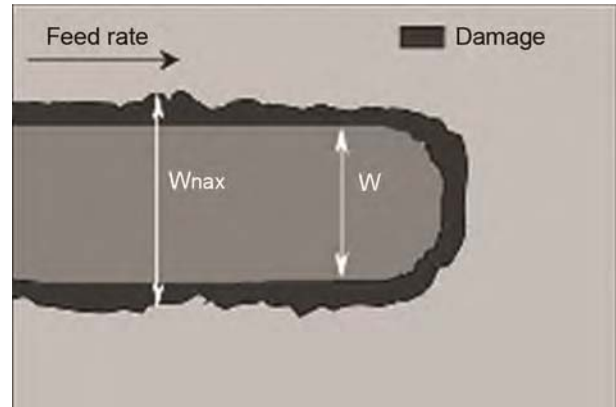


Fig. 4—Measurement of delamination

Table 4—Design table and the response (surface roughness and delamination)

Std order	Run order	Speed (m/min)	Feed (mm/min)	Depth of cut (mm)	Tool material	Surface roughness (micron)	Delamination factor
13	1	0	-1	0	-1	1.4465	1.1111
25	2	0	0	0	0	1.5845	1.6611
17	3	-1	0	0	-1	2.0311	1.6814
12	4	1	0	1	0	1.8571	1.0000
20	5	1	0	0	1	1.8571	1.4000
16	6	0	1	0	1	1.4225	1.1800
15	7	0	-1	0	1	1.0195	1.1200
19	8	-1	0	0	1	1.3911	1.6000
11	9	-1	0	1	0	1.2345	1.3000
26	10	0	0	0	0	1.7225	1.4600
5	11	0	0	-1	-1	1.1991	0.6309
23	12	0	-1	1	0	1.2755	1.4306
10	13	1	0	-1	0	0.9221	1.4600
18	14	1	0	0	-1	1.2588	1.2600
9	15	-1	0	-1	0	1.5524	0.9400
14	16	0	1	0	-1	1.9951	1.3000
24	17	0	1	1	0	1.2337	1.6288
1	18	-1	-1	0	0	1.5235	1.4800
27	19	0	0	0	0	1.5121	1.5487
7	20	0	0	-1	1	1.2081	1.6119
21	21	0	-1	-1	0	0.9813	1.7700
6	22	0	0	1	-1	1.8711	1.4800
8	23	0	0	1	1	1.1895	1.2800
2	24	1	-1	0	0	1.3831	1.2000
4	25	1	1	0	0	1.6895	1.0800
3	26	-1	1	0	0	1.8451	1.6600
22	27	0	1	-1	0	1.8261	1.4200

are large, the surface is rough; if they are small the surface is smooth. Roughness is typically considered to be the high frequency, short wavelength component of a measured surface. The surface roughness ( $R_a$ ) was evaluated using Surfcoeder SE 1700. The

measurements were made with the cut-off (0.8 mm) according to ISO as shown in Fig. 3. The results are given in Table 4.

**Measurements of delamination**

In composite and adhesively laminated structures, radiography is widely applied for the detection of defects such as fiber breakages, fiber orientation, voids, porosities and presence of foreign objects or inclusions. Thermography or infrared imaging or thermal imaging is an upcoming NDT method, which is finding increasing applications for the examination of such adhesively bonded and composite structures. The method has been used for the detection of de-laminations, de-bonds and impact damage in such structures.

The set-up for measurement of delamination using pulsed thermography was done. The computation of the delamination was done by the measurement of the maximum width of damage ( $W_{max}$ ) suffered by the material, the damage normally assigned by delamination factor ( $F_d$ ) was determined. This factor is defined as the quotient between the maximum width of damage ( $W_{max}$ ), and the width of cut ( $W$ ). The value of delamination factor ( $F_d$ ) can be obtained by the following equation:

$$F_d = W_{max} / W \quad \dots (3)$$

$W_{max}$  being the maximum width of damage in  $\mu m$  and  $W$  the width of cut in  $\mu m$ . The maximum width of damage in  $\mu m$  was obtained by the images from the Altair software as shown in Fig. 4.

A CEDIP focal plane array camera (Silver 420M) was used for experiment. The  $320 \times 240$  detector array captures the IR radiation in the 3-5  $\mu m$  spectral bands at a frame rate of up to 200 Hz. The milled composite panel was illuminated for 50 s using the

halogen lamps while the IR camera acquires the thermal images as shown in Fig. 5.

Radiography was carried out using the Balteu 160 kV industrial X-ray unit. Since the specimens to be examined had a low atomic number, low X-ray energy had to be used. The voltage and current applied during radiography was 75 kV and 21.3 mA, respectively. The measurements made in CEDIP focal plane array camera for measuring the delamination, and the values obtained using Altair software are given in Table 4.

**Artificial neural networks**

An artificial neural network (ANN), usually called neural network (NN), is a mathematical model or computational model that is inspired by the structure or functional aspects of biological neural networks. A neural network consists of an interconnected group of artificial neurons, and it processes information using a connectionist approach to computation. In most cases an ANN is an adaptive system that changes its structure based on external or internal information that flows through the network during the learning phase. Modern neural networks are non-linear statistical data modeling tools. They are usually used to model complex relationships between inputs and outputs or to find patterns in data.

A neuron is the basic element of neural networks, and its shape and size may vary depending on its duties. Analyzing neurons in terms of its activities is important, since understanding the way it works also helps us to construct the ANNs. An ANN may be seen as a black box which contains hierarchical sets of neurons producing outputs for certain inputs.

Each processing element consists of data collection, processing the data and sending the results to the relevant consequent element. The whole process may be viewed in terms of the input, weight, the summation function, and the activation function as shown in Fig. 6.

The functioning of ANNs depends on their physical structure. An ANN may be regarded as a directed graph containing a summation function, a transfer function, its structure, and the learning rule used in it. The processing element has links in between them forming a layer of networks. A neural network usually consists of an input layer, a number of hidden layers, and an output layer as shown in Fig. 6.

**Results and Discussion**

The full factorial design was used to study the effect of the four process parameters: cutting speed,

feed, depth of cut and tool material on surface roughness and delamination. The experiment includes four controllable process parameters, whose levels are presented in Table 2. An analysis of variance (ANOVA) was conducted to discern whether a difference in surface roughness and delamination between various runs is statistically significant. Tables 5 and 6 present ANOVAs results for experimental data generated during milling of GFRP. Value of “probability > *F*” less than 0.05

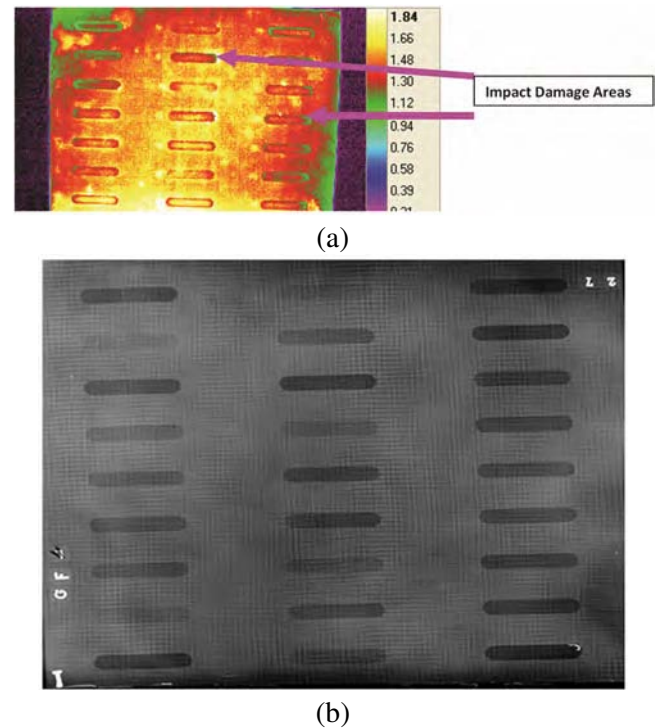


Fig. 5—Thermographic image of the composite panel clearly revealing the impact damage areas (a) before heating and (b) after heating

Table 5—Full regression analyses for surface roughness

Term	Coefficient	SE Coefficient	T	P
Constant	1.60633	0.09574	16.778	0.000
A	-0.05086	0.04787	-1.063	0.309
B	0.19853	0.04787	4.147	0.001
C	0.08103	0.04787	1.693	0.116
D	-0.1428	0.04787	-2.983	0.011
A*A	0.04777	0.0718	0.665	0.518
B*B	-0.06523	0.0718	-0.908	0.382
C*C	-0.2266	0.0718	-3.156	0.008
D*D	-0.03423	0.0718	-0.477	0.642
A*B	-0.00375	0.08291	-0.045	0.965
A*C	0.31325	0.08291	3.778	0.003
A*D	0.30949	0.08291	3.733	0.003
B*C	-0.22161	0.08291	-2.673	0.02
B*D	-0.03638	0.08291	-0.439	0.669
C*D	-0.17263	0.08291	-2.082	0.059

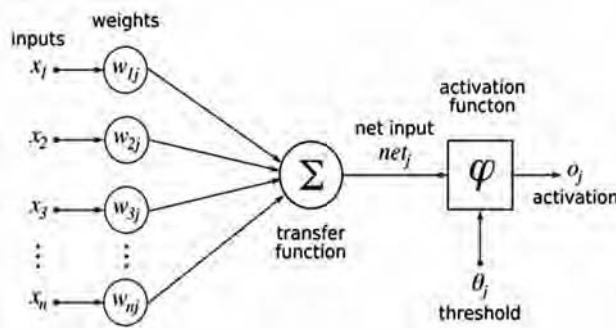


Fig. 6—Whole processing of artificial neural network

Table 6—Full regression analyses for delamination

Term	Coef	SE Coef	T	P
Constant	1.55623	0.05933	26.229	0
A	-0.14242	0.02967	-4.801	0
B	0.03773	0.02967	1.272	0.228
C	0.06568	0.02967	2.214	0.047
D	0.01659	0.02967	0.559	0.586
A*A	-0.05679	0.0445	-1.276	0.226
B*B	-0.10982	0.0445	-2.468	0.03
C*C	-0.10243	0.0445	-2.302	0.04
D*D	-0.15882	0.0445	-3.569	0.004
A*B	-0.075	0.05138	-1.46	0.17
A*C	-0.26641	0.05138	-5.185	0
A*D	0.05535	0.05138	1.077	0.303
B*C	0.06341	0.05138	1.234	0.241
B*D	-0.0325	0.05138	-0.632	0.539
C*D	-0.16262	0.05138	-3.165	0.008

Table 7—ANOVA for the reduced model on surface roughness

Source	DF	Seq SS	Adj SS	F	P
Linear terms	4	0.82752	0.20688	7.52	0.003
Interaction terms	6	1.09663	0.18277	6.65	0.003
Lack-of-fit	10	0.30710	0.03071	2.69	0.302
Pure error	2	0.02287	0.01144	-	-
Residual error	12	0.32997	0.02750	-	-
Total	26	2.62330	-	-	-

Table 8—ANOVA for the reduced model on delamination

Source	DF	Seq SS	Adj SS	F	P
Linear terms	4	0.31557	0.315567	7.47	0.003
Interaction terms	6	0.44475	0.444752	7.02	0.002
Lack-of-fit	10	0.12171	0.121708	4.85	0.183
Pure error	2	0.00502	0.005021	-	-
Residual error	12	0.12673	0.126730	-	-
Total	26	1.05097	-	-	-

indicated model terms are significant. This is desirable as it indicated that the terms in the model have significant effect on the response. Since the process is non-linear in nature the linear polynomial

will not be able to predict the response accurately therefore the second-order model (quadratic model) is used. The second-order model was postulated in obtaining the relationship between the surface roughness, delamination and the machining independent variables.

**Mathematical model for surface roughness**

The models were based on the Box-Behnkn design method. The developed second order mathematical model for surface roughness is shown in Eq. (4)

$$\begin{aligned}
 \text{Surface roughness } (R_a) = & 1.60633 - 0.05086(A) \\
 & + 0.19853(B) + 0.08103(C) - 0.14280(D) \\
 & 0.31325(A*C) + 0.30949(A*D) - 0.22161 \\
 & (B*C) - 0.17263(C*D) \dots (4)
 \end{aligned}$$

Table 7 shows the 95% confidence interval for the experiments. The analysis of variance of second-order model are shown in Table 8. For the second order model, the *P*-value for lack of fit is 0.302 (>0.05) is not significant with the lack of fit and the *F*-statistic is 2.69 (>0.05). This implies that the model could fit and it is adequate. The second order model is more precise than first-order model, because the predicted result is much more accurate than the first-order model. As well as the multiple regression coefficient of the second-order model is higher than the first-order model, i.e., 99.00 % (0.99).

The check of the normality assumptions of the data is then conducted. It can be seen from Fig. 7 that all the points on the normal plot come close to forming a straight line. This implies that the data are fairly normal and there is a no deviation from the normality. This shows the effectiveness of the developed model. All the residuals are falling on a straight line, which means that the errors are normally distributed.

The main and interaction effect plot for surface roughness has been shown in Figs 8 and 9. The plots show the variation of individual and interaction responses with the four parameters, i.e., cutting speed, feed rate, depth of cut and tool materials. In the plots, x-axis shows the value of each parameter at three levels and y-axis the response values. Horizontal line in the plot shows the mean value of the response. Figure 8 shows the main effect plot for surface roughness showing the effect of cutting speed, feed rate, depth of cut and tool material. Form the plot it can be learnt that there exists an optimal value of cutting speed and depth of cut for which the surface roughness value is minimum. Also from the plot low

value of feed gives better surface finish. Aluminium titanium nitride coated tools gives a better surface finish compared to the other two tools.

Figure 9 shows the variation of surface roughness to interaction between cutting speed and feed rate ( $v \cdot f$ ), feed rate and depth of cut ( $f \cdot d$ ) and cutting speed and depth of cut ( $v \cdot d$ ).

Eq. (4) has been used to develop a counter plot as shown in Figs 10-15. The change of surface

roughness has been observed from Figs 10-15 with respect to the variables depth of cut, cutting speed and feed rate are at their low, medium and high values. From the counter plots we can see that the cutting conditions for the respective lowest, medium and high values of cutting speeds are 100 m/min, 700 m/min and 1300 m/min, feed rates are 50 mm/min, 350 mm/min, and 650 mm/min, depth of cuts are 1 mm, 2 mm and 3 mm and tools are solid carbide, solid carbide coated with titanium nitride and aluminium titanium nitride.

Figures 10-12 show the plot of surface roughness versus depth of cut and cutting speed for the respective lowest, medium and high hold values of feed rates and tool materials. From these figures it can be observed that surface roughness value decreases with increasing cutting speed and decreasing depth of cut. Aluminium titanium nitride coated tool gives the lowest surface roughness values whereas titanium

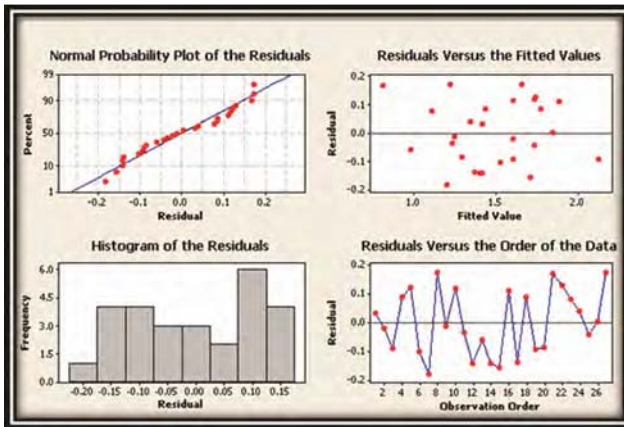


Fig. 7—Residual plot for surface roughness

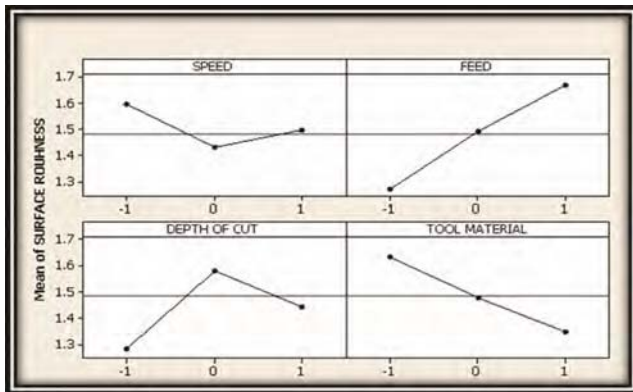


Fig. 8—Main effect plot for surface roughness

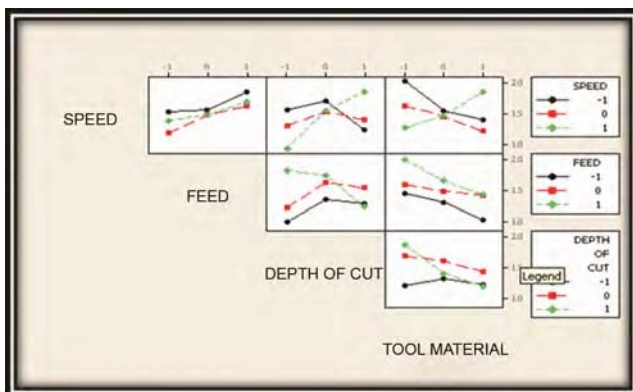


Fig. 9—Interaction plot for surface roughness

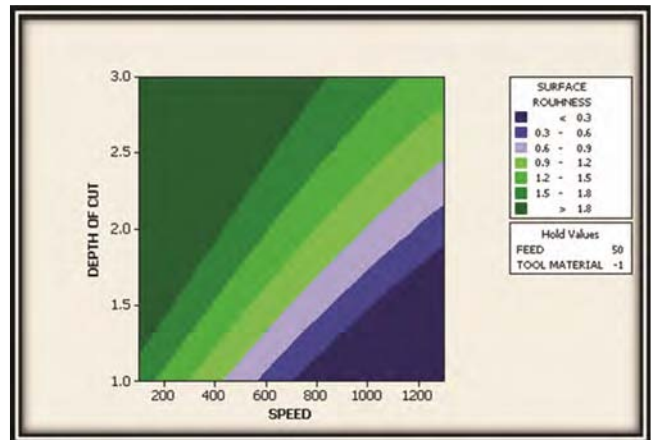


Fig. 10—Contour plot of surface roughness vs depth of cut, speed (low)

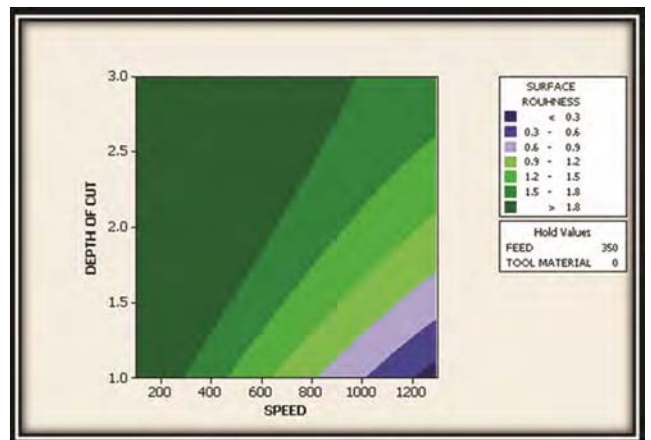


Fig. 11—Contour plot of surface roughness vs depth of cut, speed (medium)

nitride coated tools yield higher values of surface roughness. Solid carbide gives the highest values of surface roughness among the three tools.

Figures 13-15 show the plot of surface roughness versus depth of cut and feed rate for the respective lowest, medium and high hold values of cutting speeds and tool materials. Figures 13-15 show that a surface roughness value decreases with increasing feed rate and decreasing depth of cut. Aluminium titanium nitride coated tool gives the lowest surface roughness values whereas titanium nitride coated tools yield higher values of surface roughness. Solid carbide gives the highest values of surface roughness among the three tools.

**Mathematical model for delamination**

The models were based on the Box-Behnken design method. The developed second-order mathematical model for delamination is shown in Eq. (5)

$$\begin{aligned}
 \text{Delamination } (F_d) = & 1.55623 - 0.14242(A) \\
 & + 0.03773(B) + 0.06568(C) + 0.01659(D) \\
 & - 0.26641(A * C) + 0.05535(A * D) + 0.06341(B * C) \\
 & - 0.16262(C * D) \dots (5)
 \end{aligned}$$

Table 8 shows the analysis of variance of second-order model with 95% confidence interval for the delamination experiments.

The check of the normality assumptions of the data is then conducted. It can be seen from Fig. 16 that all the points on the normal plot come close to forming a straight line. This implies that the data are fairly normal and there is a no deviation from the normality. This shows the effectiveness of the developed model. All the residuals are falling on a straight line, which means that the errors are normally distributed.

The main and interaction effect plot for delamination has been shown in Figs 17 and 18. The plots show the variation of individual and interaction responses with the four parameters, i.e., cutting speed, feed rate, depth of cut and tool materials. In the plots, x-axis shows the value of each parameter at three levels and y-axis the response values. Horizontal line in the plot shows the mean value of the response. Figure 17 shows the main effect plot for delamination showing the effect of cutting speed, feed rate, depth of cut and tool material. Form the plot it can be learnt that delamination decreases with decrease in feed and depth of cut. This plot also shows that delamination decreases with increase in cutting speed. Less damage is obtained using coated tools rather than uncoated tool.

Figure 18 shows the variation of delamination to interaction between cutting speed and feed rate ( $v * f$ ), feed rate and depth of cut ( $f * d$ ) and cutting speed and depth of cut ( $v * d$ ).

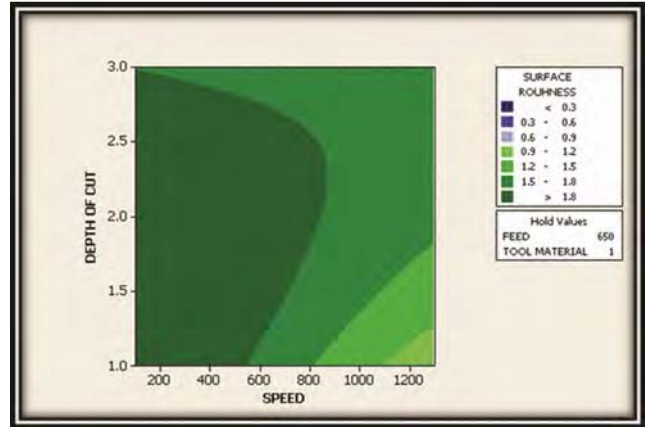


Fig. 12—Contour plot of surface roughness vs depth of cut, speed (high)

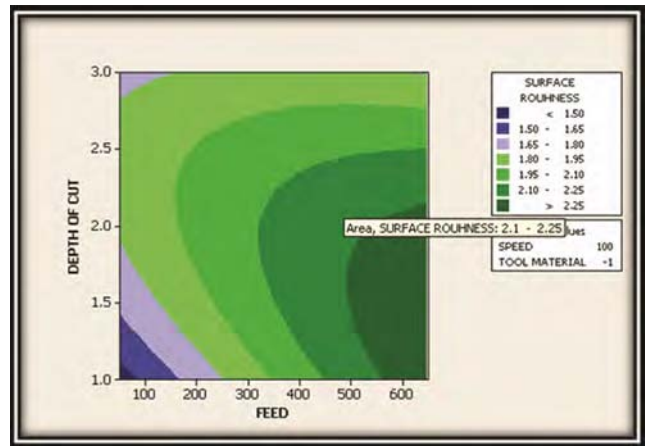


Fig. 13—Contour plot of surface roughness vs depth of cut, feed (low)

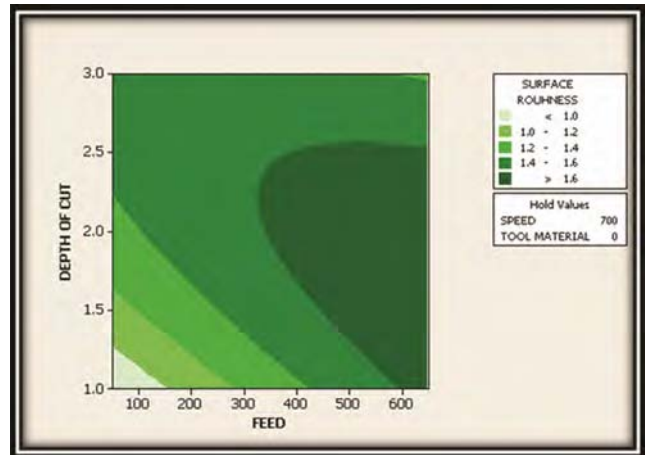


Fig. 14—Contour plot of surface roughness vs depth of cut, feed (medium)

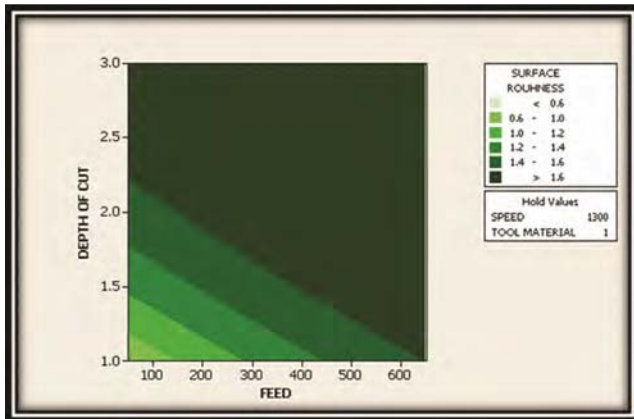


Fig. 15—Contour plot of surface roughness vs depth of cut, feed (high)

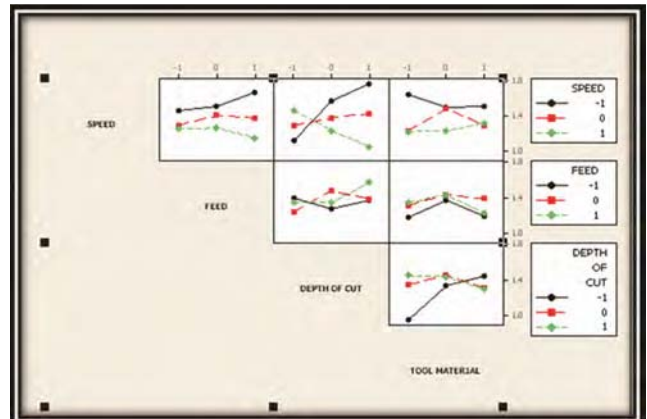


Fig. 18—Interaction plot for delamination

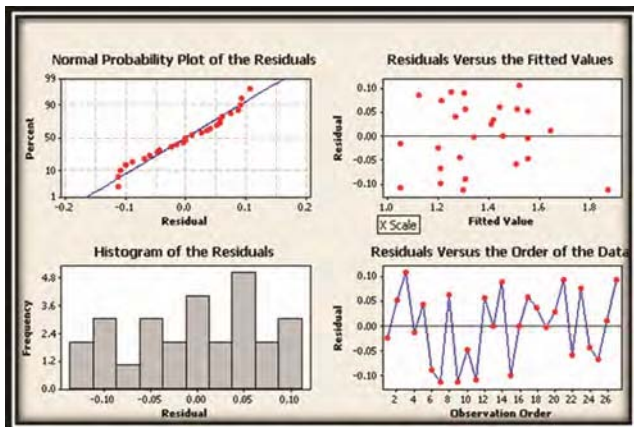


Fig. 16—Residual plot for delamination

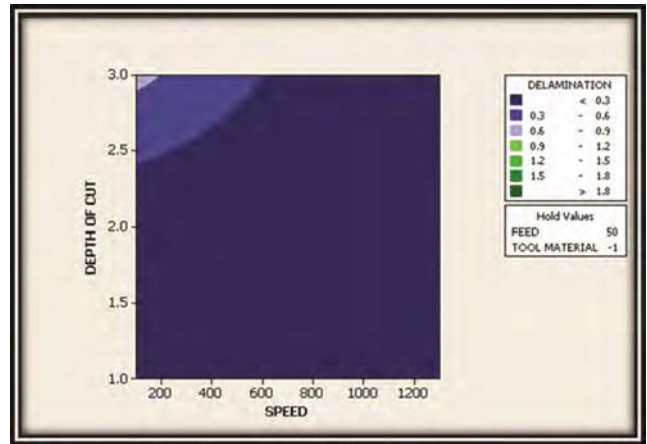


Fig. 19—Contour plot of delamination vs depth of cut, speed (low)

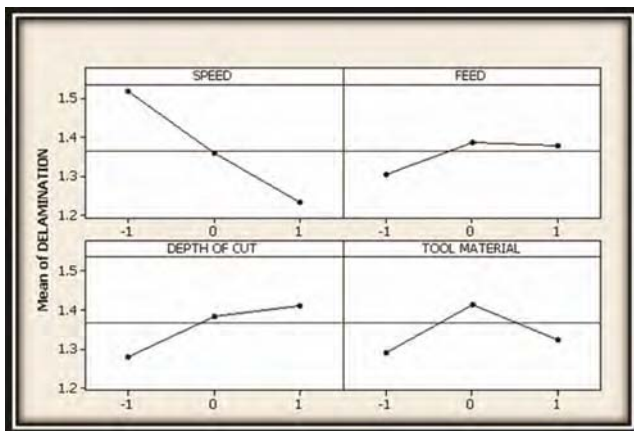


Fig. 17—Main effect plot for delamination

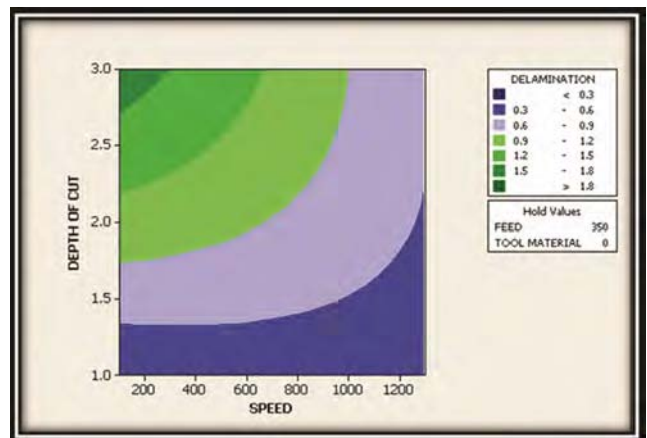


Fig. 20—Contour plot of delamination vs depth of cut, speed (medium)

Eq. (5) has been used to develop a counter plot as shown in Figs 19-24, the changes of delamination have been observed in these figures with respect to the variables depth of cut, cutting speed and feed rate are at their lowest, medium and high values. From the counter plots we can see that the cutting conditions for the respective lowest, medium and high values of cutting

speeds are 100 m/min, 700 m/min and 1300 m/min, feed rates are 50 mm/min, 350 mm/min, and 650 mm/min, depth of cuts are 1 mm, 2 mm and 3 mm and tool materials are solid carbide, titanium nitride coated and aluminium titanium nitride coated.

Figures 19-21 show the plot of surface roughness versus depth of cut and cutting speed for the

respective lowest, medium and high hold values of feed rates and tool materials. It can be observed from these figures that delamination value decreases with increasing cutting speed and decreasing depth of cut. Aluminium titanium nitride coated tool gives the lowest delamination values.

Figures 22-24 show the plot of delamination versus depth of cut and feed rate for the respective lowest, medium and high hold values of cutting speeds and tool materials. It can be observed from these figures that a delamination value decreases with increasing feed rate and decreasing depth of cut. Aluminium titanium nitride coated tool gives the lowest surface roughness values.

**ANN approach**

Training of neural network model was performed using twenty seven experimental data. Neurons in the input layer correspond to depth of cut, feed, speeds and tools used. The output layer corresponds to

surface roughness and delamination. In this model, the inputs are fully connected to the outputs. In order to train the network a proper selection of training and learning function are to be made. Training function and learning functions are mathematical procedures used to automatically adjust the network's weights and biases in order to train the network model. The training function dictates a global algorithm that affects all the weights and biases of a given network. The learning function can be applied to individual weights and biases within a network. There are numerous algorithms available for training neural network models. The training functions trainlm, traingd, traingdm and traingda used in the training the network model were selected on the basis of trial and error. Trainlm is a network training function that updates weight and bias values according to Levenberg-Marquardt optimization algorithm. Traingd is a network training function that updates weight and bias values according to gradient descent

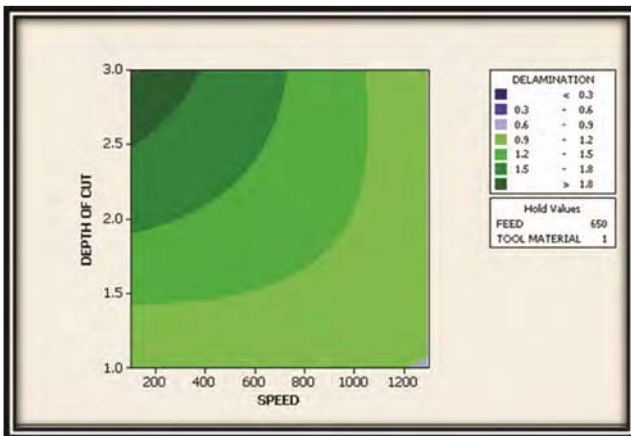


Fig. 21—Contour plot of delamination vs depth of cut, speed (high)

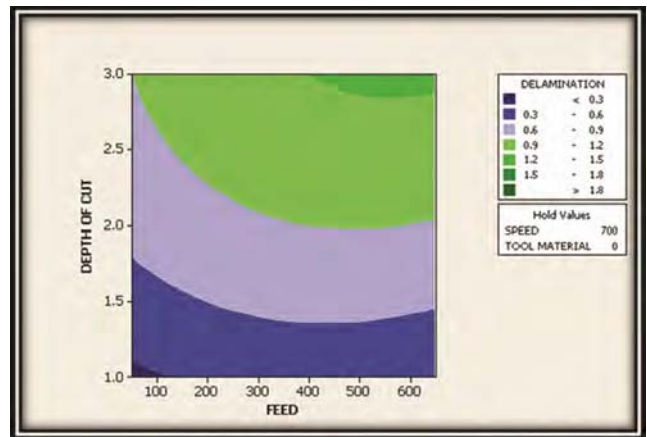


Fig. 23—Contour plot of delamination vs depth of cut, feed (medium)

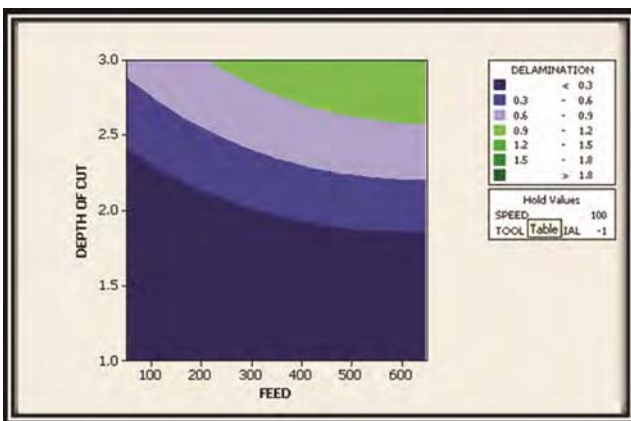


Fig. 22—Contour plot of delamination vs depth of cut, feed (low)

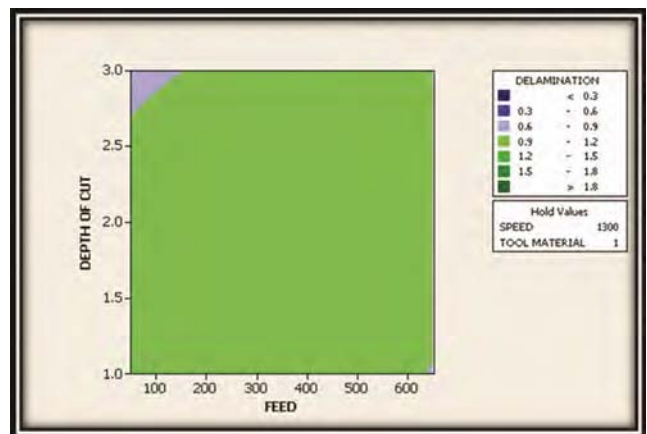


Fig. 24—Contour plot of delamination vs depth of cut, feed (high)

Table 9—Comparison of ANN predictions with training data set

Test	Surface roughness			Delamination		
	Expt output	ANN output	Error	Expt output	ANN output	Error
1	1.4465	1.4465	-2.04689E-07	1.17611	1.176108	2.05155E-06
2	1.5845	1.54513	0.039369937	1.60812	1.735229	-0.12710905
3	2.031	2.031	0	1.62876	1.628765	-4.9816E-06
4	1.857	1.857004	-3.7872E-06	1.03923	1.039226	4.30251E-06
5	1.857	1.857004	-3.7872E-06	1.31133	1.31133	-3.6616E-07
6	1.4225	1.4225	3.156E-08	1.21968	1.21968	-7.2027E-08
7	1.0195	1.019504	-4.08476E-06	1.18599	1.185993	-2.956E-06
8	1.39119	1.39119	3.156E-07	1.50509	1.505086	4.09623E-06
9	1.2345	1.234501	-7.84491E-07	1.758	1.758	0
10	1.7225	1.932003	-0.209502922	1.50812	1.390239	0.117880901
11	1.199	1.198999	8.56628E-07	0.94164	0.94164	0
12	1.2755	1.275501	-1.27142E-06	1.36459	1.36459	-1.6414E-08
13	0.922	0.922	0	1.45444	1.454438	1.50865E-06
14	1.25884	1.258836	3.81425E-06	1.21359	1.21359	-1.8374E-07
15	1.55248	1.552484	-4.34626E-06	1.10756	1.107557	2.66598E-06
16	1.995	1.994997	3.35437E-06	1.33979	1.33979	4.92528E-07
17	1.2337	1.233698	1.95672E-06	1.56793	1.567928	2.40825E-06
18	1.5235	1.5235	-4.59874E-08	1.45424	1.454239	1.48856E-06
19	1.512	1.341882	0.170118359	1.55247	1.543242	0.009227855
20	1.208	1.208	1.80343E-08	1.43452	1.434516	3.50777E-06
21	0.98135	0.981353	-3.36339E-06	1.395	1.394996	3.53814E-06
22	1.871	1.871002	-1.75834E-06	1.44697	1.446968	2.25832E-06
23	1.1895	1.189497	3.40848E-06	1.28935	1.289355	-4.574E-06
24	1.383	1.383	3.7872E-07	1.24012	1.240116	3.98109E-06
25	1.6895	1.6895	1.53291E-07	1.1413	1.141297	3.05502E-06
26	1.845	1.845003	-2.66907E-06	1.65542	1.655419	6.96261E-07
27	1.826	1.825998	2.43463E-06	1.34469	1.34469	-1.5287E-08

Table 10—Tested data

Test No.	Speed	Feed	Depth of Cut	Tool use	Surface	Delamination
1	29	360	1	1	1.39119	1.31133
2	43	540	1.5	2	1.234501	1.21968
3	58	720	2	2	1.932003	1.185993
4	39	450	1.25	3	1.198999	1.505086

Table 11—Comparison of ANN predictions with tested data set

Tested no.	Surface roughness			Delamination		
	Expt output	ANN output	Error	Expt output	ANN output	Error
1	1.39119	1.37119	0.02	1.31133	1.35226	-0.04
2	1.234501	1.244501	-0.01	1.21968	1.25133	-0.03
3	1.932003	1.882003	0.05	1.185993	1.16968	0.01
4	1.198999	1.188999	0.01	1.505086	1.49805	0.00

algorithm. Traingdm is a network training function that updates weight and bias values according to gradient descent with momentum. Traingda is a network training function that updates weight and bias values according to gradient descent with adaptive learning rate. The transfer functions used in training

Table 12—Times taken and performance

Performance (%)	TRAIN LM	TRAIN GD	TRAINGDM	TRAINGDA
	98	96	95	89
	Time taken, h			
TANSIG	1.45	2	2.35	3
PURELIN				
LOGSIG	2.15	2.45	2.50	4.15
PURELIN				

the network are liner transfer function purelin, tansig and sigmoid transfer function logsig. After training of the network, the model was tested using other experimental data points, which were not used in the training process. The results predicted from the ANN model are compared with those obtained by experimental test in Table 9. It is also found that ANN prediction is in good agreement with the experimental results. The simulation test values are shown in Table 10 and the compared values are given in Table 11. Besides, a comparison of various training algorithms and squashing functions are shown in Table 12. From

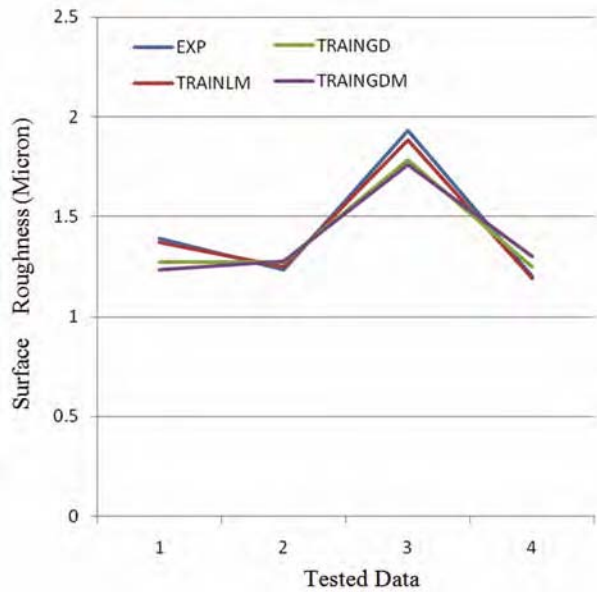


Fig. 25—Comparison of tested data and surface roughness with various algorithms

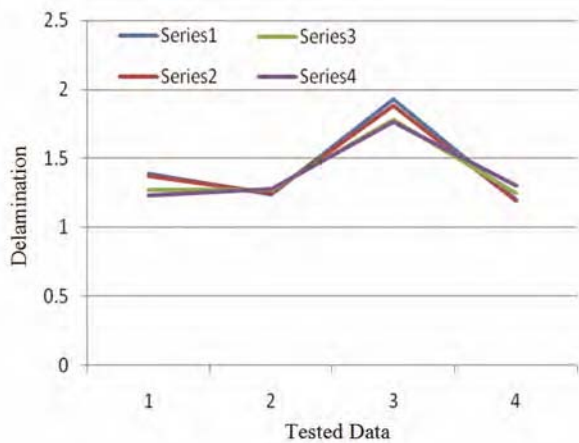


Fig. 26—Comparison of tested data and delamination factor with various algorithms

Table 12 it is found that TRAINLM, tansig and purelin are best in predicting the model with respect to the performance and computational time. Figure 25 shows the comparison between the simulated values and experimental output for various training algorithms. From Fig. 25 it can be inferred that TRAINLM predicts the experimental results more accurately compared to other algorithms in case of surface roughness. Figure 26 shows the comparison between the simulated values and experimental output for various training algorithms. From Fig. 26 it can be inferred that TRAINLM also predicts the experimental results more accurately compared to other algorithms in case of delamination.

### Conclusions

An experimental approach to the evaluation of surface roughness and delamination caused by various tools using response surface methodology was proposed in this study. A mathematical model was developed to predict the surface roughness and delamination for milling epoxy based GFRP composites. This technique is convenient to predict the effects of different influential combinations of machining parameters by conducting minimum number of experiments. Cutting speed and depth of cut was found to be the most influential parameter among the main factors in case of surface roughness, whereas feed rate and tools material are more influential parameter among the main factors in case of delamination. In addition to the main factors, the interactions between cutting speed and depth of cut, cutting speed and tool material, feed rate and depth of cut, depth of cut and tool material were found to be more significant for both surface roughness and delamination than the linear terms contrary to the findings of many authors. Thus, further investigations are recommended in this direction. For all hold values of feed and tool material, the surface roughness is low when the cutting speed is high and depth of cut is low. For all hold values of cutting speed and tool materials, the surface roughness is low when the feed rate is low and depth of cut is also low. For all hold values of feed and tool material, there exists an optimal value of cutting speed and depth of cut for which the delamination value is less. For all hold values of cutting speed and tool materials, the delamination is low when the feed rate is low and depth of cut is also low. The results show the suitability of solid carbide for number of industrial applications by carefully selecting the appropriate values for cutting parameters. For precise and good surface finish coated tool performs better than uncoated tool.

In this study the experimental observations were incorporated into the ANN multi objective model. A feed forward back propagation neural network was developed to predict surface roughness and delamination. It is found that the developed ANN model has good interpolation capability and can be used as an efficient predictive model for good surface roughness and less damage (delamination). Increasing the number of nodes increases the computational cost and decreases the error.

### Acknowledgement

The authors are thankful to IGCAR, Kalpakkam, Tamil Nadu, India for the help rendered in conducting the experiments.

### References

- 1 Koenig W C, Grass P & Willerscheid H, *Ann CIRP*, 34 (1985) 537-548.
- 2 Komanduri R, *ASME Mech Eng*, 114 (1993) 58-644
- 3 Ramulu M, Wern C W & Garbini G L, *Compos Manuf*, 4 (1) (1993) 39-51.
- 4 Erisken E, *Int J Mach Tools Manuf*, 39 (1999) 1611-1618.
- 5 Mukherjee I & Ray P K, *Comput Ind Eng*, 50 (2006) 15-34.
- 6 Benardos P G & Vosniakos G C, *Int J Mach Tools & Manuf*, 43 (2003) 833-844.
- 7 Hasmi M S J, *J Mater Process Technol*, 56 (1996) 54-65.
- 8 Alauddin M, El Baradie M A & Hashmi M S J, *J Mater Process Technol*, 55(2) (1995) 123-127.
- 9 Reddy N & Rao P V, *Int J Adv Manuf Technol*, 26 (2005) 1202-1210.
- 10 Lou S J & Chen J C, *Int J Adv Manuf Technol*, 15 (3) (1999) 200-209.
- 11 Chiang S T, Liu D I, Lee A C & Chieng W H, *Int J Mach Tools Manuf*, 35(4) (1995), 637-660.
- 12 Luo T, Lu W, Krishnamurthy K & McMillin B, *Int J Mach Tools Manuf*, 38 (1998) 1343.
- 13 Rangwala S S & Dornfeld D A, *IEEE Trans Syst Man Cyber*, 19 (1989) 299-317.
- 14 Kohli A & Dixit U S, *Int J Adv Manuf Technol*, 25(1-2) (2005) 118-129.
- 15 Aggarwal A & Singh H, *Sadhana*, 30(6) (2005) 699-711.
- 16 Chandrasekaran M, Muralidhar M, Krishna C M & Dixit U S, *Int J Adv Manuf Technol*, 46(5-8) (2010) 445-464.
- 17 Box G E P & Wilson K B, *J Royal Stat Soc Ser B*, 13(1) (1951) 1-45.